

Effects of back pressure on the superplastic forming of domes

SONG YU-QUAN, KOU SHU-QING

Materials Engineering Department, Jilin University of Technology, Changchun 130025, People's Republic of China

Z.C. WANG

Materials Science Centre, University of Manchester and UMIST, Grosvenor Street, Manchester M1 7HS, UK

The stress state during "simple" superplastic bulge forming (without a back pressure) is different from that when a back pressure is applied. In the former procedure, specimens or components are deformed under a biaxial tensile stress state, while in the latter, the deformation is achieved under the combination of a biaxial tensile stress and a uniaxial compressive stress state. Both theoretical and experimental studies have shown that when a back pressure is present, the deformation cannot be treated as simply governed by the difference between the forming pressure and the back pressure. The analytical expressions for the forming relationships and the influence of back pressure on experimental m - $\log \dot{\epsilon}_e$ (where m is the strain-rate sensitivity and $\dot{\epsilon}_e$ is the equivalent tensile strain rate for bulge forming) relationships for Zn-22 wt % Al and Zn-4 wt % Al-1 wt % Cu are given. Results show that with increasing back pressure, the m - $\log \dot{\epsilon}_e$ curve shifted towards higher strain rates, but the maximum m values were not affected.

1. Introduction

Superplastic forming of metallic sheet materials is attracting increasing interest in commercial practice, particularly in the aerospace industry. However, most superplastic materials cavitate during high-temperature deformation, which deteriorates the post-forming properties of the components. The most effective way of controlling cavitation is to superimpose a hydrostatic pressure during deformation [1]. Uniaxial tensile testing is usually involved in the fundamental studies for the evaluation of superplastic deformation properties, such as the relationship between strain rate sensitivity, m , and strain rate, $\dot{\epsilon}$, (m - $\log \dot{\epsilon}$ curves).

Bulge forming of domes is usually adopted as the early stages of many commercial superplastic forming processes [2]. However, most work on the determination of the optimum procedure for bulge forming has been based on the analyses of stress-strain rate relationships and the optimum procedure has been predicted from the strain rate corresponding to the maximum value of strain-rate sensitivity obtained from uniaxial tension. Both theoretical and experimental investigations [3–7] have shown that the m - $\log \dot{\epsilon}$ curve obtained by uniaxial tensile testing may not accord with that obtained by biaxial tensile (bulge) testing. The determination of m - $\log \dot{\epsilon}$ curves under free bulge-forming conditions (without a back pressure) have been reported previously [8]. The stress state during superplastic bulge forming without a back

pressure is different from that when a back pressure is applied. In the former procedure, specimens are deformed under a biaxial tensile stress state, in the latter, the deformation is achieved under both biaxial tensile and uniaxial compressive stress state. As the m value is related to stress states and microstructure [9], the m - $\log \dot{\epsilon}$ curves for bulge forming will also be affected by the application of a back pressure (or hydrostatic pressure). In practice, it is more useful to determine the m - $\log \dot{\epsilon}$ relationship by biaxial tensile test rather than by uniaxial tensile test. The present paper is concerned with the analytical solutions for the forming relationships and the determination of the experimental m - $\log \dot{\epsilon}_e$ (where $\dot{\epsilon}_e$ is the equivalent tensile strain rate for bulge forming) curves. Materials used for experimental investigations were Zn-22 wt % Al (Zn-22Al) and Zn-4 wt % Al-1 wt % Cu (Zn-4Al-1Cu) cross-rolled sheets.

2. Theory

2.1. Geometric relationships and basic assumptions

A superplastically bulged dome under hydrostatic pressure is illustrated in Fig. 1, in which r_0 is the die radius, P_f is the applied forming pressure, P_b is the back pressure and other symbols are as illustrated. For simplicity, the following assumptions were made.

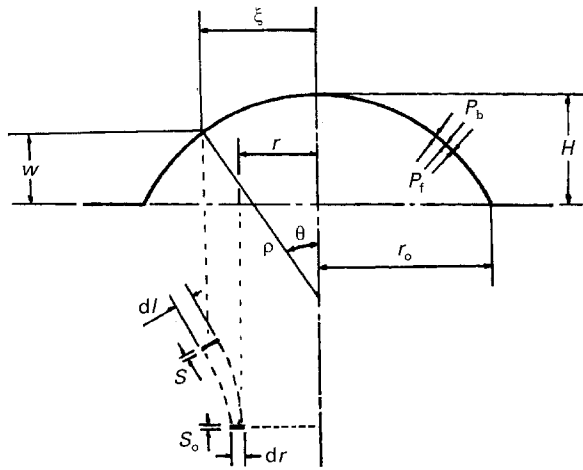


Figure 1 Schematic illustration of a bulged dome.

1. The material is completely plastic and incompressible.
2. When the dome height, H , is equal to the die radius, r_0 , the surface area of a dome is twice that of the base, corresponding to an equivalent tensile strain of 100% [10], which is sufficient for most commercial applications. For this reason, only $H \leq r_0$ is considered. Consequently, the geometry of the median plane of the formed dome is equivalent to part of a sphere at any instant during deformation.
3. At the periphery, the diaphragm is rigidly clamped.
4. Anisotropy only exists in the thickness direction.
5. $P_b \gg (P_f - P_b)$, the stress gradient along thickness direction is neglected.
6. Cavitation or bending during deformation is neglected.

Because different stress levels bring about non-uniform thickness along the dome profile, the dome is divided into finite concentric rings, which were further divided by a group of planes through the axis of the dome, Fig. 2. The following relationships can be obtained from Figs 1 and 2.

$$\sin \theta = \xi / \rho \quad (1a)$$

$$\cos \theta = d\xi / dl \quad (1b)$$

$$\xi \cdot d\gamma = \rho d\alpha \quad (1c)$$

$$(\rho^2 - \xi^2)^{1/2} = \rho - (H - w) \quad (2a)$$

$$\rho = (\xi_0^2 + H^2) / 2H \quad (2b)$$

where θ is the subtend angle of any finite ring whose radius changed from the original value, r , to the current value, ξ , and thickness changed from original value of S_0 to the current thickness, S , ρ is the radius of the dome and the rest are as illustrated in Figs 1 and 2.

2.2. Mechanical relationships

The three principle stresses at any point of the dome will be the tangential stress, σ_t ; the circumferential stress, σ_c , and the radial stress (or thickness stress), σ_r . From Figs 1 and 2, the following equations can be obtained.

$$\pi \xi^2 (P_f - P_b) = 2\pi \xi S \sigma_t \sin \theta \quad (3)$$

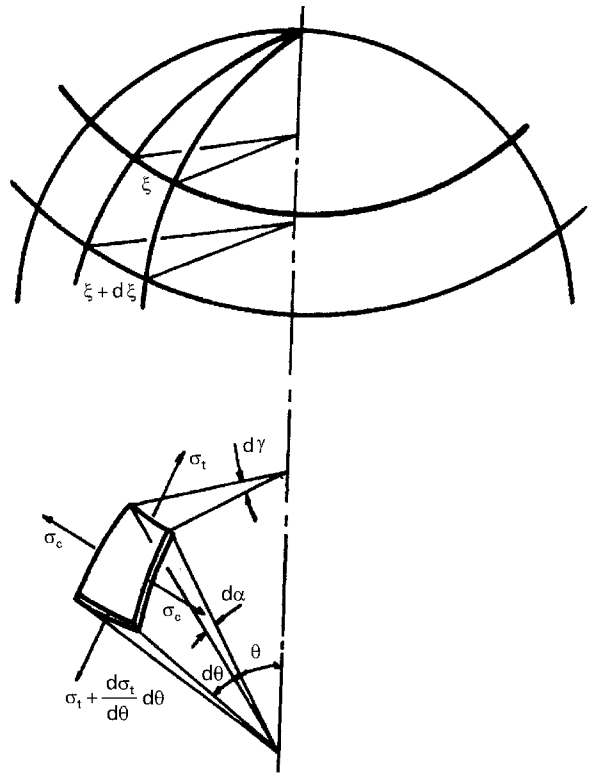


Figure 2 Schematic illustration of a finite portion of a dome used for mechanical analyses.

$$(P_f - P_b) \xi \sin(d\gamma) \rho \sin(d\theta) = \left(\sigma_t + \frac{\partial \sigma_t}{\partial \theta} d\theta \right) (\xi + d\xi) S(d\gamma) \sin \frac{d\theta}{2} + \sigma_t \xi S(d\gamma) \sin \frac{d\theta}{2} + 2\sigma_c \rho S(d\theta) \sin \frac{d\alpha}{2} \quad (4)$$

Substituting $\sin \theta = \xi / \rho$ in Equation 1 into Equation 3 gives

$$\sigma_t = \rho (P_f - P_b) / 2S \quad (5)$$

In Equation 4, using $\sin(d\gamma) \approx d\gamma$, $\sin(d\theta) \approx d\theta$, $\sin(d\alpha/2) \approx d\alpha/2$, etc., and neglecting the high orders of finite components, σ_c is obtained as

$$\sigma_c \approx \rho (P_f - P_b) / 2S \quad (6)$$

It is seen that through those approximations, σ_c is about the same as σ_t . In fact, σ_c is equal to σ_t at the apex and half of that value at the bottom. The radial stress, σ_r , is $-P_b$. Corresponding to the three principle stresses, the three principle strains are defined as tangential strain $\epsilon_t = \ln(dl/dr)$, circumferential strain $\epsilon_c = \ln(\xi/r)$ and radial (or thickness) strain $\epsilon_r = \ln(S/S_0)$.

According to the incremental theory [11], the equivalent stress, σ_e , and the equivalent strain rate, $\dot{\epsilon}_e$, can be expressed as

$$\sigma_e = \left\{ \frac{R}{1+R} (\sigma_t - \sigma_c)^2 + \frac{1}{1+R} [(\sigma_c - \sigma_r)^2 + (\sigma_r - \sigma_t)^2] \right\}^{1/2} \quad (7)$$

$$\dot{\epsilon}_e = \frac{1+R}{(1+2R)^{1/2}} \left(\dot{\epsilon}_t^2 + \frac{2R}{1+R} \dot{\epsilon}_t \dot{\epsilon}_c + \dot{\epsilon}_c^2 \right)^{1/2} \quad (8)$$

where R is the coefficient of anisotropy along the thickness direction, $\dot{\varepsilon}_t$ and $\dot{\varepsilon}_c$ are tangential and circumferential strain rates, respectively.

As the circumferential stress, σ_c , is approximated to be the same as the tangential stress, σ_t , the corresponding strains and strain rates will be also approximately the same, i.e. $\varepsilon_c = \varepsilon_t$ and $\dot{\varepsilon}_c = \dot{\varepsilon}_t$. Assuming that the material is incompressible, the following equation can be obtained

$$\begin{aligned}\varepsilon_c &= \varepsilon_t \\ &= -\frac{\varepsilon_r}{2}\end{aligned}\quad (9)$$

Combining the definitions of the three principle strains and Equation 9 gives

$$\begin{aligned}\frac{dl}{dr} &= \frac{\xi}{r} \\ &= \left(\frac{S_0}{S}\right)^{1/2}\end{aligned}\quad (10)$$

$$\frac{dr}{r} = \frac{dl}{\xi}\quad (11)$$

Substituting Equation 1 into Equation 11 and integrating using boundary conditions of $\xi = r_0$ when $r = r_0$, and using Equation 2 gives

$$\frac{\xi}{r} = 1 + \frac{W}{2Q - H} = 1 + \frac{Hw}{r_0^2} = \frac{r_0^2(r_0^2 + H^2)}{r_0^4 + H^2r^2}\quad (12)$$

Let $h = H/r_0$ and $y = w/r_0$, Equation 12 gives

$$\frac{\xi}{r} = 1 + hy\quad (13)$$

$$y = \frac{h(r_0^2 - r^2)}{r_0^2 + h^2r^2}\quad (14)$$

The thickness variation along the dome height can be derived from Equations 14 and 11 as

$$S = S_0(1 + hy)^{-2}\quad (15)$$

Similarly, the stresses, strain rates and strains in the three principle directions can be expressed as the functions of h and y

$$\sigma_c = \sigma_t = \frac{r_0(P_f - P_b)}{4S_0} \frac{1 + h^2}{h} (1 + hy)^2\quad (16a)$$

$$\sigma_r = -P_b\quad (16b)$$

$$\dot{\varepsilon}_c = \dot{\varepsilon}_t = \frac{2y}{1 + h} \frac{dh}{dt}\quad (17a)$$

$$\dot{\varepsilon}_r = -\frac{4y}{1 + h} \frac{dh}{dt}\quad (17b)$$

$$\begin{aligned}\varepsilon_c &= \varepsilon_t \\ &= \ln(1 + hy)\end{aligned}\quad (18a)$$

$$\varepsilon_r = \ln(1 + hy)^{-2}\quad (18b)$$

where dt is a very small time interval over which the dimensionless dome height, h , increased to $h + dh$. The equivalent stress and strain rate at the apex can be

obtained by substituting Equations 16 and 17 into Equations 7 and 8, respectively, and also $h = y$ at the dome apex, gives

$$\sigma_e = \left(\frac{2}{1 + R}\right)^{1/2} \left[\frac{r_0(P_f - P_b)}{4S_0} \frac{(1 + h^2)^3}{h} + P_b \right]\quad (19a)$$

$$\dot{\varepsilon}_e = [2(1 + R)]^{1/2} \frac{2h}{1 + h^2} \frac{dh}{dt}\quad (19b)$$

2.3. Measurement of m

From the definition [6] of $m = d \log \sigma_e / d \log \dot{\varepsilon}_e$, the velocity of dome height $V = dH/dt$ and Equation 19, the m value during superplastic bulge forming under the application of a back pressure is given by the following equation

$$m = \frac{d \log [(P_f - P_b)(r_0^2 + H^2)^3 / (4S_0 r_0^4 H) + P_b]}{d \log V - d \log (r_0^2 + H^2) + d \log H}\quad (20)$$

For convenience during experimental measurements, Equation 20 can be written in the differential form. Let $P = P_f - P_b$, after a small time interval of dt , the pressure difference, P , dome apex velocity and dome height changed from P_1, V_1 and H_1 to P_2, V_2 and H_2 . For the constant back pressure condition, m can be expressed as

$$m \approx \frac{\log [(BP_2 + P_b) / (AP_1 + P_b)]}{\log [V_2 H_2 (r_0^2 + H_1^2) / V_1 H_1 (r_0^2 + H_2^2)]}\quad (21)$$

where $A = (r_0^2 + H_1^2)^3 / (4S_0 r_0^4 H_1)$ and $B = (r_0^2 + H_2^2)^3 / (4S_0 r_0^4 H_2)$. When two specimens are used for the determination of m , each of the specimens can be bulged to the same height, e.g. H_1 , then Equation 21 can be simplified as

$$m \approx \frac{\log [(AP_2 + P_b) / (AP_1 + P_b)]}{\log (V_2 / V_1)}\quad (22)$$

Equation 22 is used for the measurement of m during bulge forming by the pressure jump method using two specimens.

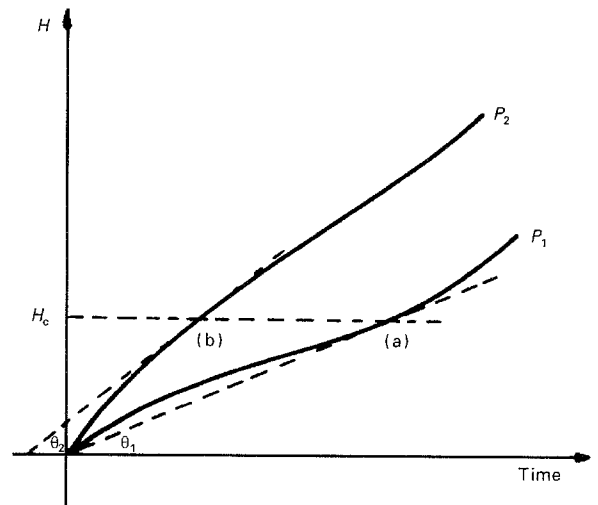


Figure 3 Schematic illustration of the pressure jump method used to determine m during superplastic bulge forming.

TABLE I The measurement of the m values for Zn-22Al under various back pressures during superplastic bulge forming of domes (dome height $H = 34.28$ mm)

P_b (MPa)	P_1 (MPa)	P_2 (MPa)	V_1 (mm s ⁻¹)	V_2 (mm s ⁻¹)	$\dot{\epsilon}_e$ (s ⁻¹)	m
0	0.1	0.2	0.006	0.078	1.99×10^{-4}	0.27
	0.2	0.3	0.078	0.209	2.59×10^{-3}	0.41
	0.3	0.4	0.209	0.340	6.93×10^{-3}	0.59
	0.4	0.5	0.340	0.450	1.13×10^{-2}	0.79
	0.5	0.6	0.450	0.574	1.46×10^{-2}	0.74
	0.6	0.7	0.574	0.835	1.86×10^{-2}	0.41
	0.7	0.8	0.835	1.843	2.73×10^{-2}	0.16
1.8	0.1	0.2	0.037	0.151	1.22×10^{-3}	0.34
	0.2	0.3	0.151	0.309	5.01×10^{-3}	0.45
	0.3	0.4	0.309	0.436	1.02×10^{-2}	0.71
	0.4	0.5	0.436	0.557	1.45×10^{-2}	0.80
	0.5	0.6	0.557	0.693	1.85×10^{-2}	0.75
	0.6	0.7	0.693	0.869	2.30×10^{-2}	0.62
	0.7	0.8	0.869	1.224	2.88×10^{-2}	0.36
2.3	0.1	0.2	0.070	0.246	2.30×10^{-3}	0.35
	0.2	0.3	0.246	0.466	8.17×10^{-3}	0.48
	0.3	0.4	0.466	0.645	1.55×10^{-2}	0.72
	0.4	0.5	0.645	0.815	2.14×10^{-2}	0.81
	0.5	0.6	0.815	1.010	2.70×10^{-2}	0.74
	0.6	0.7	1.010	1.275	3.35×10^{-2}	0.59
	0.7	0.8	1.275	1.752	4.23×10^{-2}	0.38
3.0	0.1	0.2	0.159	0.456	5.28×10^{-3}	0.38
	0.2	0.3	0.456	0.850	1.51×10^{-2}	0.46
	0.3	0.4	0.850	1.120	2.82×10^{-2}	0.80
	0.4	0.5	1.120	1.390	3.72×10^{-2}	0.84
	0.5	0.6	1.390	1.724	4.61×10^{-2}	0.71
	0.6	0.7	1.724	2.205	5.72×10^{-2}	0.54
	0.7	0.8	2.205	3.113	7.30×10^{-2}	0.34

TABLE II The measurement of the m values for Zn-4Al-1Cu under various back pressures during superplastic bulge forming of domes (dome height $H = 35$ mm)

P_b (MPa)	P_1 (MPa)	P_2 (MPa)	V_1 (mm s ⁻¹)	V_2 (mm s ⁻¹)	$\dot{\epsilon}_e$ (s ⁻¹)	m
0	0.075	0.1	0.013	0.032	4.38×10^{-4}	0.32
	0.1	0.15	0.032	0.063	1.08×10^{-3}	0.60
	0.15	0.25	0.063	0.120	2.12×10^{-3}	0.79
	0.25	0.4	0.120	0.240	4.05×10^{-3}	0.68
	0.4	0.6	0.240	0.530	8.09×10^{-3}	0.51
	0.6	0.8	0.530	1.120	1.78×10^{-2}	0.38
2.0	0.075	0.1	0.039	0.059	1.31×10^{-3}	0.44
	0.1	0.15	0.059	0.089	2.00×10^{-3}	0.70
	0.15	0.25	0.089	0.148	3.00×10^{-3}	0.79
	0.25	0.4	0.148	0.280	4.99×10^{-3}	0.63
	0.4	0.6	0.280	0.560	9.44×10^{-3}	0.53
	0.6	0.8	0.560	1.040	1.89×10^{-2}	0.43
3.0	0.075	0.1	0.076	0.105	2.56×10^{-3}	0.47
	0.1	0.15	0.105	0.150	3.54×10^{-3}	0.70
	0.15	0.25	0.150	0.237	5.06×10^{-3}	0.80
	0.25	0.4	0.237	0.417	7.99×10^{-3}	0.67
	0.4	0.6	0.417	0.750	1.41×10^{-2}	0.60
	0.6	0.8	0.750	1.260	2.53×10^{-2}	0.50

3. Experiment and discussion

The two-specimen, pressure jump method [12] was used to study back-pressure influence on the relationship between m and $\log \dot{\epsilon}_e$. Cross-rolled superplastic sheets of Zn-22Al and Zn-4Al-1Cu were used as test materials. Specimens were 200 mm square plates of 1.5 mm thickness. The anisotropy along the thickness

direction of the two materials was measured as $R = 0.58$ for Zn-22Al and $R = 0.61$ for Zn-4Al-1Cu. The die radius was 50 mm. Testing started after holding for 12 min at 523 K for Zn-22Al and 593 K for Zn-4Al-1Cu. In order to avoid the local stress and temperature inhomogeneity caused by the direct contact of a pin and a dome apex in the

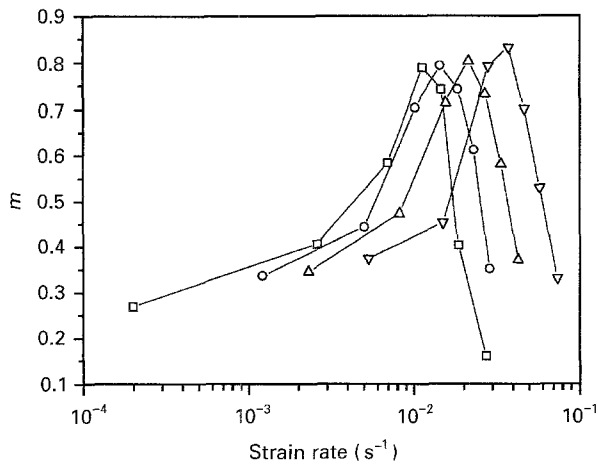


Figure 4 The effects of back pressure on the m - $\log \dot{\epsilon}_e$ curve for Zn-22Al during superplastic bulge forming. Back pressure: (□) 0 MPa, (○) 1.8 MPa, (△) 2.3 MPa, (▽) 3.0 MPa.

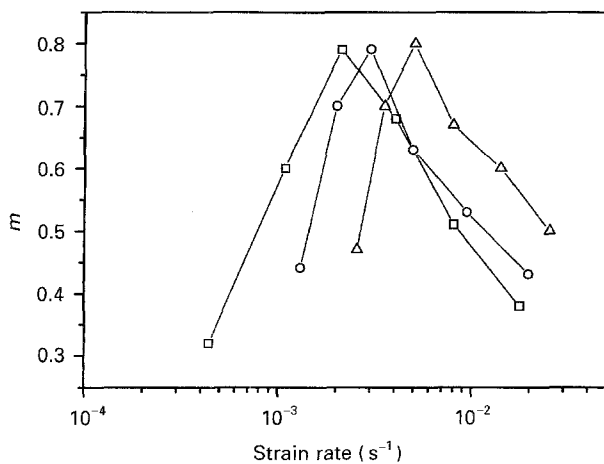


Figure 5 The effects of back pressure on the m - $\log \dot{\epsilon}_e$ curve for Zn-4Al-1Cu during superplastic bulge forming. Back pressure: (□) 0.0 MPa, (○) 2.0 MPa, (△) 3.0 MPa.

conventional technique for measuring dome height, the computerized, photoelectric measuring system for bulge forming testing described elsewhere [8] has been modified to include a back pressure system.

The dome height-time, ($H-t$), curves (Fig. 3) for each specimen was recorded during testing. The tangential of the curve at any point is the velocity of the dome apex. From Equation 22, m values can be calculated. The experimental data for the two materials under various back pressures and forming pressures are listed in Tables I and II.

The m - $\log \dot{\epsilon}_e$ curves for each material are plotted in Figs 4 and 5. It is seen that with increasing back pressure, the m - $\log \dot{\epsilon}_e$ curve moves to higher strain rates, while the maximum m values remain essentially the same. This suggests that a higher strain rate may be used when a back pressure is applied during superplastic forming.

4. Conclusion

The application of a back pressure during superplastic forming of domes changes the stress state from biaxial tension to the combination of a biaxial tension and a uniaxial compression stress state. Both theoretical analyses and experimental results showed that back pressure has an influence on m . Experimental results on Zn-22Al and Zn-4Al-1Cu have shown that the m - $\log \dot{\epsilon}_e$ curve shifted towards higher strain rates with increasing back pressure, but the maximum m value was not affected. This suggests that with the application of a back pressure, the optimum forming strain rate can be increased.

References

1. N. RIDLEY and Z.C. WANG, *Mater. Sci. Forum*, **170** (1994) 177.
2. J. PILLING and N. RIDLEY, in "Superplasticity in Crystalline Solids" (The Institute of Metals, London, 1989) p. 160.
3. H.S. YANG, H.K. AHMED and W.T. ROBERTS, *Mater. Sci. Eng.* **A122** (1989) 193.
4. Z.J. LOU, *Forg. Technol.* **3** (1986) 7 (in Chinese).
5. D.J. ZHOU, J. LIAN and M. SUERY, *Mater. Sci. Technol.* **4** (1988) 348.
6. SONG YU-QUAN and LIAN SHUJUN, *Chinese Sci. Bull.* **35** (1990) 73.
7. *Idem.*, *Sci. China (A)* **4** (1990) 440.
8. SONG YU-QUAN and Z.C. WANG, *Mater. Sci. Technol.* **9** (1993) 57.
9. Z.X. GUO and N. RIDLEY, *Mater. Sci. Eng.* **A114** (1989) 97.
10. I-WEI CHEN and LIANG AN XUE, *J. Am. Ceram. Soc.* **73** (1990) 2585.
11. N.M. WANG and M.R. SHAMMAMY, *J. Mech. Phys. Solids* **17** (1969) 43.
12. SONG YUQUAN and ZHAOJUN, *Mater. Sci. Eng.* **84** (1986) 111.

Received 16 June
and accepted 25 November 1994